BJ www.biochemj.org

BJ Structure

Biochem. J. (2009) **417**, 55–64 (Printed in Great Britain) doi:10.1042/BJ20071702

Characterization of the activity and folding of the glutathione transferase from *Escherichia coli* and the roles of residues Cys[10] and His[106]

Xin-Yu WANG*†, Zai-Rong ZHANG*‡ and Sarah PERRETT*[1]

*National Laboratory of Biomacromolecules, Institute of Biophysics, Chinese Academy of Sciences, 15 Datun Road, Chaoyang District, Beijing 100101, People's Republic of China, †Department of Biophysics, Institute of Physics, Nankai University, 94 Weijin Road, Tianjin 300071, People's Republic of China, and ‡Graduate University of the Chinese Academy of Sciences, 19 Yuquan Road, Shijingshan District, Beijing 100049, People's Republic of China

GSTs (glutathione transferases) are an important class of enzymes involved in cellular detoxification. GSTs are found in all classes of organisms and are implicated in resistance towards drugs, pesticides, herbicides and antibiotics. The activity, structure and folding, particularly of eukaryotic GSTs, have therefore been widely studied. The crystal structure of EGST (GST from *Escherichia coli*) was reported around 10 years ago and it suggested Cys[10] and His[106] as potential catalytic residues. However, the role of these residues in catalysis has not been further investigated, nor have the folding properties of the protein been described. In the present study we investigated the contributions of residues Cys[10] and His[106] to the activity and stability of EGST. We found that EGST shows a complex equilibrium unfolding profile, involving a population of at least two partially folded intermediates, one of which is dimeric. Mutation of residues Cys[10] and His[106] leads to stabilization of the protein and affects the apparent steady-state kinetic parameters for enzyme catalysis. The results suggest that the imidazole ring of His[106] plays an important role in the catalytic mechanism of the enzyme, whereas Cys[10] is involved in binding of the substrate, glutathione. Engineering of the Cys[10] site can be used to increase both the stability and GST activity of EGST. However, in addition to GST activity, we discovered that EGST also possesses thiol:disulfide oxidoreductase activity, for which the residue Cys[10] plays an essential role. Further, tryptophan quenching experiments indicate that a mixed disulfide is formed between the free thiol group of Cys[10] and the substrate, glutathione.

Key words: enzyme activity, glutathione transferase (GST), protein folding, protein structure.

INTRODUCTION

GSTs (glutathione transferases; EC 2.5.1.18) are a large family of enzymes involved in cellular detoxification; they catalyse the reduction of electrophilic substrates into non-harmful compounds utilizing GSH (for reviews, see [1–5]). GSTs are dimeric, and each subunit contains two domains: a thioredoxin-like domain containing the G-site (i.e. GSH-binding site) and an all-α-domain containing the H-site (or hydrophobic binding site). GST structures have been divided on the basis of their structure, activity and other characteristics into a number of classes, including Alpha [6], Beta [7], Delta [8], Epsilon [9], Zeta [10], Theta [11], Mu [6], Pi [6], Sigma [12] and Omega [13] classes. Interestingly, the sequence similarity between different classes is low, but the overall architectures are very similar. Although a great deal of data regarding the structure and function of GSTs is available, most studies to date have focused on the GSTs of eukaryotes. GSTs of prokaryotes, particularly bacterial GSTs, for which the Beta class is named, have been less well studied. To date, the most extensively studied Beta-class GST is PmGST (GSTB1-1 from *Proteus mirabilis*) [7,14–20]. Another example is EGST (*Escherichia coli* GST), which was likewise identified around 15 years ago [21] and its crystal structure has been determined in two crystal forms [22,23]. EGST has 53 % sequence identity with PmGST, and most proline residues are conserved between the two proteins (Figure 1). Another protein, Ure2p, a prion protein found in yeast, also adopts a GST fold and its structure is strikingly similar to that of EGST [24], although the two proteins have only 17.4 % sequence similarity. Given the similarity in folded structure between these proteins, it is worthwhile to determine the extent to which the folding properties are also similar. Although the folding properties of Ure2p have been studied in some detail (reviewed in [25]), the folding of EGST has not yet been studied. The folding mechanisms of GST proteins studied to date show various extents of complexity, ranging from a simple two-state model [26,27], a population of a single clearly defined intermediate compatible with a three-state model [28–30] and a few examples of more complicated folding mechanisms [31–34]. The folding mechanism of GSTs, in particular the population of a dimeric versus a monomeric intermediate, has been suggested to reflect structural differences between family members, particularly the packing of the dimer interface [31,35–38]. In the present study we apply a variety of spectroscopic probes of structure, namely CD, intrinsic fluorescence and the binding of the hydrophobic probe ANS (8-anilinonaphthalene-1-sulfonic acid), to examine the equilibrium folding properties of EGST.

The activity of the well-characterized eukaryotic GST enzymes of Alpha, Pi and Mu classes invariably depends on the presence of an N-terminal tyrosine residue, which is generally replaced in Theta-class enzymes by a serine residue, also situated near the N-terminus [1,2]. Theta-class GSTs, which are found over a broad spectrum of organisms, show huge diversity in substrate specificity as well as variation in location or type of catalytic residue. Bacterial enzymes, where the N-terminal tyrosine/serine residue is replaced by a cysteine residue, were initially grouped under the Theta class, but have subsequently been recognized as a novel distinct class termed Beta [7]. In the crystal structure

Abbreviations used: ANS, 8-anilinonaphthalene-1-sulfonic acid; CDNB, 1-chloro-2,4-dinitrobenzene; CSM, centre of spectral mass; EGST, *Escherichia coli* glutathione transferase; GdmCl, guanidinium chloride; GR, glutathione reductase; GST, glutathione transferase (formerly termed glutathione *S*-transferase); HEDS, bis-(2-hydroxyethyl) disulfide; PmGST, GSTB1-1 from *Proteus mirabilis*; WT, wild-type.

[1] To whom correspondence should be addressed (email sarah.perrett@iname.com).

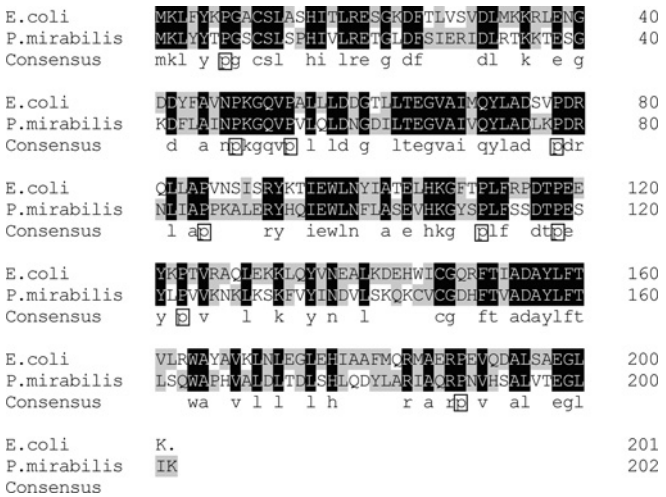

Figure 1 Sequence alignment of EGST and PmGST

The Figure was generated using DNAMAN (Lynnon Corp., Vaudreuil-Dorion, QC, Canada). The α-helical regions are as follows: α1 (Leu^{12}–Gly^{22}), α2 (Gly^{66}–Asp^{75}), α3 (Arg^{91}–Glu^{104}), α4 (Pro^{123}–^{Glu}/$_{Gln}$^{143}), α5 (Ala^{154}–Trp^{164}), α6 (Leu^{175}–Arg^{188}) and α7 (Val^{191}–Glu^{198}). Nine proline residues are conserved between the two proteins. Of these, Pro^{7}, Pro^{78}, Pro^{85}, Pro^{123} and Pro^{189} are near the end of a helix. The first two and the last α-helix segments of the proteins are very similar; the differences between the proteins lie mainly in regions α5 and α7.

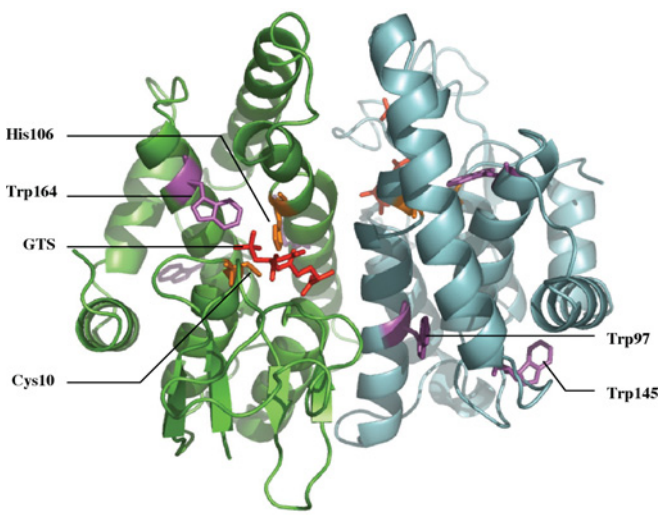

Figure 2 Schematic representation of EGST structure

The Figure was generated using the Protein Data Base entry 1a0f [22] and the program PyMOL [50]. The A (green) and B (cyan) chains of the homodimer are shown. The location of the three tryptophan residues at positions 97, 145 and 164 (magenta) and the positions of Cys^{10} (Cys10) and His^{106} (His106) orange) are indicated. GTS, the inhibitor glutathione sulfonate (red) bound in the active site.

of EGST (Figure 2), the active site is occupied by the inhibitor glutathione sulfonate, and the only residues that are close to the sulfonyl group of the inhibitor are Cys^{10} and His^{106} [22]. It was suggested that the amide N atom of Cys^{10} might act as a hydrogen-bond donor to stabilize the activated thiolate form of GSH when bound as substrate. Alternatively, it was also considered possible that the Cys^{10} S$^{\gamma}$ atom might interact directly with the GSH thiol [22].

In the present study we mutated Cys^{10} to alanine and serine, and residue His^{106} to alanine and phenylalanine, and then examined the effect of mutation on the stability and activity of the protein. Our results suggest that the aromatic ring of His^{106} plays an important role in the catalytic mechanism of the enzyme, whereas the side chain at position 10 is associated with the binding of the substrate, GSH. Although replacement of Cys^{10} or His^{106} by other amino acid residues allows a certain amount of GST activity to be maintained, we discovered that EGST also possesses thiol:disulfide oxidoreductase activity for which the presence of cysteine at position 10 is essential.

EXPERIMENTAL

Materials

GSH, Tris base and Tris/HCl were from Sigma–Aldrich. GdmCl (guanidinium chloride) and urea were from ICN. Other chemicals were local products of analytical grade. Molecular-biology enzymes were from TaKaRa. Solutions were prepared volumetrically; the concentration of GdmCl solutions was confirmed using an Abbe refractometer. Double-deionized water was used throughout.

Expression and protein purification

WT (wild-type) EGST cDNA was cloned from *E. coli* strain TG2 into the vector mini-pRSETa (a gift from Dr Mark Bycroft, Centre for Protein Engineering, Cambridge, U.K.) between the BamHI and EcoRI sites, using the following primers (listed 5′ to 3′):

GGCCGCGGATCCATGAAATTGTTCTACAAACCGGGTG

CCGCCGGAATTCCTATTACTTTAAGCCTTCCGC

The mutants C10A, C10S, H106A, H106F, W97A, W97F, W145A, W145F, W164A and W164F were constructed by PCR, ligated into the mini-pRSETa vector between the BamHI and HindIII restriction sites and verified by DNA sequencing. The target genes were expressed in *E. coli* host strain C41 [39]. Cells were grown in Luria-Bertani medium containing 0.1 mg/ml ampicillin at 37 °C with shaking at 200 rev./min in an Innova 4330 incubator. After at least 12 h of growth, cells were harvested by centrifugation at 2000 ***g*** for 30 min at 4 °C, resuspended in McAc-10 [20 mM Tris/HCl, 300 mM NaCl, 10 mM imidazole and 10 % (v/v) glycerol, pH 8.0], sonicated [120 bursts of 6 s each interspersed by 9 s pauses, using a JY92-II sonicator (Scientz Biotechnology Co. Ltd, Ningbo, China) set at 200 W] and then centrifuged at 30000 ***g*** for 30 min at 4 °C. The expression products contain a 17-residue peptide tag containing hexahistidine (MRGSHHHHHHGLVPRGS) at the N-terminus. The supernatant was loaded onto a column containing nickel-affinity resin [Chelating Sepharose Fast Flow; Amersham International (now GE Healthcare)] pre-equilibrated with McAc-10. After washing with 10 column vol. of McAc-10 and then 10 column vol. of McAc-70 (McAc buffer containing 70 mM imidazole) until the A_{280} was constant, the bound GST protein was then eluted with McAc-250 (McAc buffer containing 250 mM imidazole). After elution, the protein was dialysed against 50 mM Tris/HCl buffer, pH 7.5, 8.0 or 8.4, containing 200 mM NaCl, or 100 mM sodium phosphate buffer, pH 6.5 or 7.5, and flash-frozen for storage at −80 °C. The protein was judged to be > 95 % pure by SDS/15%-(w/v)-PAGE. The concentration of EGST in terms of monomers was determined by A_{280} using an absorption coefficient of 28590 $M^{-1} \cdot cm^{-1}$, calculated using the method of Gill and von Hippel [40].

Table 1 Apparent steady-state kinetic parameters for WT and mutant EGST using GSH and CDNB as substrates

The conditions were as follows: temperature, 25 °C; buffer, 100 mM phosphate, pH 6.5; protein concentration, 0.75 μM. Measurements were taken as described in the Experimental section (note that the maximum concentration of substrate that could be used was limited by solubility). Results are the mean ± S.E.M. for at least three independent measurements.

	GSH (CDNB 2 mM)			CDNB (GSH 5 mM)		
EGST	K_m (mM)	k_{cat} (s^{-1})	k_{cat}/K_m ($s^{-1} \cdot mM^{-1}$)	K_m (mM)	k_{cat} (s^{-1})	k_{cat}/K_m ($s^{-1} \cdot mM^{-1}$)
WT	0.3 ± 0.1	7.7 ± 1.4	25.7 ± 9.7	1.9 ± 0.2	9.1 ± 1.4	4.8 ± 0.9
C10A	2.5 ± 0.5	41.0 ± 6.5	16.4 ± 4.2	4.3 ± 0.6	55.8 ± 5.4	13.0 ± 2.2
C10S	0.05 ± 0.01	0.3 ± 0.1	6.0 ± 2.3	4.4 ± 0.3	1.6 ± 0.3	0.4 ± 0.1
H106A	1.4 ± 0.3	1.1 ± 0.1	0.8 ± 0.2	1.3 ± 0.2	1.1 ± 0.1	0.8 ± 0.2
H106F	1.9 ± 0.4	6.8 ± 2.6	3.6 ± 1.6	2.1 ± 0.2	4.8 ± 0.4	2.3 ± 0.3

Assay of GST activity

All enzyme assays were performed at 25 °C using a Shimadzu UV-2501PC spectrometer. The GST activity of WT and mutant EGST was determined using CDNB (1-chloro-2,4-dinitrobenzene) as the substrate, as described by Habig and Jakoby [41]. To determine the apparent kinetic parameters, the concentration of one substrate was varied while the other was kept constant and the data were analysed as Lineweaver–Burk plots. The final reaction system contained 0.2–5.0 mM GSH, 0.2–2.0 mM CDNB, different concentrations of EGST protein and either 100 mM phosphate buffer, pH 6.5, without NaCl, or 50 mM Tris/HCl buffer, pH 7.5, containing 200 mM NaCl.

Assay of thiol:disulfide oxidoreductase activity

The thiol:disulfide oxidoreductase activity of EGST was assayed by a coupled GR (glutathione reductase)/NADPH reaction monitored by UV absorption at 340 nm as described by Axelsson et al. [42]. The volume of the reaction system was 1 ml, containing 100 mM sodium phosphate, pH 7.5, 1 mM EDTA, 0.15 mM NADPH, 0.24 units/ml GR, 0.2–1.5 mM GSH and 0.2–5 mM HEDS [bis-(2-hydroxyethyl) disulfide]. The final protein concentration was 0.75 μM and the measurements were performed at 25 °C. The reaction was initiated by addition of EGST.

Intrinsic-fluorescence measurements

All fluorescence measurements were performed as described in [43] at 25 °C in a thermostatically controlled cuvette using a Hitachi F-4500 or a Shimadzu RF-5301PC spectrofluorimeter. For unfolding experiments, the protein samples containing different concentrations of denaturant was pre-equilibrated at 25 °C for at least 12 h before measurements were taken. In refolding experiments, the proteins were first denatured in 8 M GdmCl for about 8 h; the fully denatured protein was then diluted to give different final concentrations of GdmCl and pre-incubated for 12 h, as for the unfolding experiments. Excitation was at 280 nm and emission spectra were monitored between 300 and 400 nm. Excitation and emission slit widths were adjusted according to the protein concentration within the range 2.5–5.0 nm. The maximum change in intensity on denaturation was observed at 337 nm, which was therefore used to monitor the change in fluorescence intensity over the course of denaturation. Data were also represented as the CSM (centre of spectral mass) [44], which is sensitive to the change in the maximum emission wavelength. In the case of EGST, the profiles when plotting the CSM or the maximum wavelength of emission (λ_{max}) were the same (results not shown), but the CSM profile has reduced 'noise', so was used in preference. The final concentration of protein in the denaturation samples was 0.5–10 μM (of monomer). The chemical denaturant used was GdmCl or urea. Fitting of the data was carried out using a three-state model:

$N_2 \leftrightarrow I_2 \leftrightarrow 2U$ ([33] and references cited therein)

where N_2 is the native dimer, I_2 is a partially unfolded dimeric intermediate and U is the fully denatured state, based on the observation that the second unfolding transition shows protein-concentration-dependence, whereas the first transition does not (see the Results section and the Discussion below).

ANS binding fluorescence

ANS was added to the protein solution to give a 100-fold excess over the concentration of protein. Excitation was at 397 nm and the emission spectra were recorded between 420 and 600 nm after incubation at 25 °C for 2 h in the dark. The ANS fluorescence of a protein-free blank was subtracted for each sample at each concentration of GdmCl, and the emission value was relative to the intensity of ANS in the presence of protein but in the absence of GdmCl. The maximum change in emission on unfolding was observed at 480 nm.

CD spectroscopy

CD spectra were measured at 25 °C in a 0.1-cm-path-length thermostatically controlled cuvette using a Pistar-180 instrument (Applied Photophysics). The spectra were acquired using a 1 nm step size and 2 nm slit widths.

RESULTS

Effect of mutation of the key residues Cys[10] and His[106] on the GST activity of EGST

In order to investigate the role of Cys^{10} and His^{106} in the structure and function of EGST, we constructed the mutants C10A, C10S, H106A and H106F. The activity of these mutants towards GSH with the standard GST substrate CDNB was measured and the steady-state kinetic constants were compared with those of WT EGST in Table 1. C10A showed a 5- or 6-fold higher k_{cat} than WT for both GSH and CDNB, accompanied by an 8-fold increase in the K_m for GSH. Conversely, C10S showed a 25-fold lower k_{cat} for GSH (and 5-fold lower k_{cat} for CDNB) than WT, but, interestingly, this was accompanied by a 6-fold decrease in the K_m for GSH. It seems that increased polarity of the side chain results in tighter binding to GSH, but lower activity, suggesting that the presence of a cysteine residue at position 10 may represent a compromise between efficient substrate binding and efficient product release.

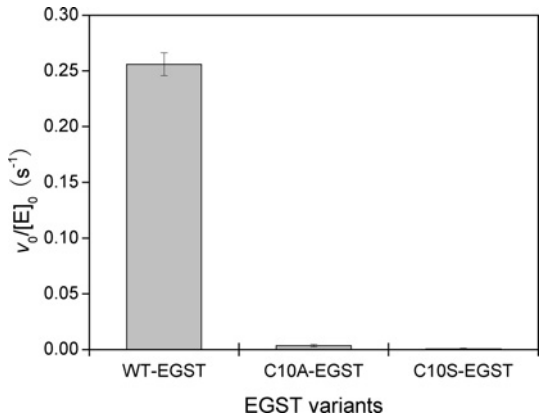

Figure 3 Comparison of GSH-dependent disulfide oxidoreductase activity of WT EGST and its mutants C10A and C10S

The experimental conditions were: temperature, 25 °C; pH, 7.5; buffer, 100 mM phosphate. The substrate concentrations were 1 mM GSH and 5 mM HEDS. Other conditions were as described in the Experimental section.

The case of H106A and H106F is simpler, in that both showed an increase in the K_m for GSH and no obvious change in the K_m for CDNB. H106A showed clearly decreased activity compared with WT, whereas the decrease in activity for H106F was less obvious. None of the Cys^{10} and His^{106} mutations described here fully abrogated the GST activity of EGST.

Cys^{10} is essential for EGST thiol:disulfide oxidoreductase activity

Given that the closely related bacterial enzyme PmGST possesses thiol:disulfide oxidoreductase activity, involving the equivalent residue Cys^{10} [17], we tested to see whether EGST also shows this activity. As shown in Figure 3, EGST is able to use GSH to reduce the substrate HEDS. Furthermore, this thiol:disulfide oxidoreductase activity depends on the presence of a cysteine residue at position 10 in EGST. The mutations C10S and C10A both destroy this activity, suggesting involvement of the free thiol group in the reaction mechanism, consistent with the reaction mechanism for PmGST, which involves formation of a mixed disulfide with GSH [7,17].

Cys^{10} can form a disulfide bond with GSH in the active site of EGST

In order to further investigate the reaction mechanism of the thiol:disulfide oxidoreductase activity of EGST, we constructed a series of mutants where each of the three tryptophan residues of EGST (Trp^{97}, Trp^{145} and Trp^{164}) was replaced in turn by alanine or phenylalanine. We then looked for tryptophan quenching in the presence of GSSG, which would be an indication of mixed-disulfide formation [45]. As shown in Figure 4, addition of GSSG to WT EGST caused a decrease in the intrinsic tryptophan fluorescence excited at 295 nm (Figure 4A). In the case of the Trp^{97} and Trp^{145} mutants (W97A, W97F, W145A and W145F), the reduction in tryptophan fluorescence was more pronounced (Figure 4B and results not shown). In each case, this change was partly reversed by further addition of GSH (Figures 4A and 4B and results not shown). Mutations at position 164 (i.e. W164A or W164F) or position 10 greatly weakened the quenching effect of GSSG (Figure 4C and results not shown). These results indicate that the observed quenching phenomenon involves the residues Cys^{10} and Trp^{164}. It is known that proximity of a disulfide bond can lead to quenching of tryptophan fluorescence [45]. Thus these results suggest that a disulfide bond forms between Cys^{10} and GSH, which then quenches the fluorescence of the nearby Trp^{164}

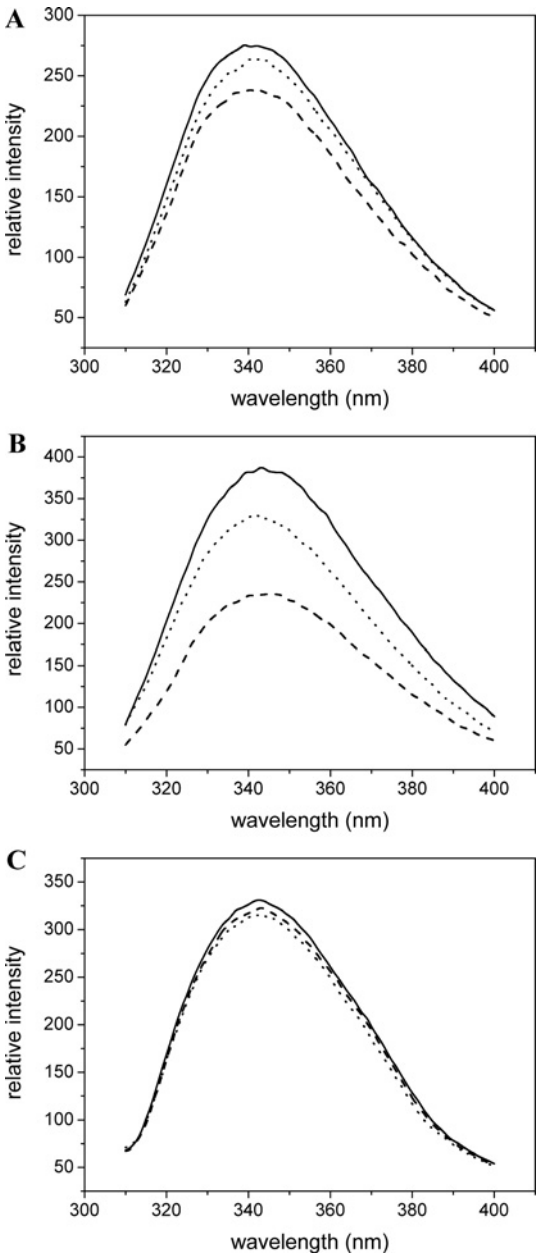

Figure 4 Comparison of the effect of GSSG and GSH on the tryptophan fluorescence of EGST

The intrinsic fluorescence of tryptophan was excited at 295 nm. The experimental conditions were: pH, 7.5; temperature, 25 °C; buffer, 50 mM Tris/HCl + 200 mM NaCl. The final concentration of the protein was about 2 μM and was adjusted so that the initial fluorescence intensities were similar for all mutants. The final GSSG and GSH concentrations were 50 and 100 μM respectively. Spectra were acquired in the following order: continuous line, protein only; broken line, addition of GSSG; dotted line, addition of GSH. The initial volume of the sample was 800 μl, and 20 μl of GSH or GSSG was added in each case. (**A**) WT EGST; (**B**) W97A; (**C**) C10A. The results for similar cases are not shown: W97F, W145A and W145F were similar to W97A; W164A and W164F were similar to C10A.

(Figure 2). The quenching effect would be expected to be less pronounced for WT EGST (where two tryptrophan residues in addition to Trp^{164} contribute to the total instrinsic fluorescence signal) compared with Trp^{97} or Trp^{145} mutants (which contain only one additional tryptophan residue). The fact that the structurally conservative phenylalanine mutants show the same result as the alanine mutants indicates that replacement of the tryptophan

residues does not introduce any significant structural change in the protein, and this was confirmed by comparison of their far-UV CD spectra (results not shown).

Investigation of WT EGST folding and stability

In order to determine how Cys^{10} and His^{106} contribute to the structure and stability of the protein, we examined the folding properties of WT EGST and compared this with the folding and stability of its mutants. We performed folding and unfolding experiments at pH 7.5, 8.0 and 8.4 at 25 °C using GdmCl as the denaturant and monitored the intrinsic fluorescence (Figure 5A). Two unfolding transitions were observed, indicating population of an intermediate, and the first transition was shifted to lower GdmCl concentration with increasing pH value. The two transitions are observed more clearly when the fluorescence data are represented as the CSM (Figure 5B; see the Experimental section) than when plotting the fluorescence signal at a single wavelength (Figure 5A).

We observed that the denaturation process is fully reversible at pH 7.5 (Figure 5C), a pH value at which the protein is also most stable (Figure 5A). This demonstrates that the observed folding transitions are genuinely at equilibrium, and it is therefore possible, in principle, to obtain meaningful thermodynamic parameters from the unfolding curves under these conditions. We therefore adopted pH 7.5 as the standard condition for further folding experiments.

In order to determine at what point in the denaturation process dissociation of the dimer occurs, we examined the protein-concentration-dependence of the unfolding transitions. As shown in Figure 6A, the midpoint of the second transition shifts to higher GdmCl concentration when the protein concentration is increased, whereas the first transition remains essentially unaffected. This then indicates that EGST partially unfolds to form a dimeric intermediate during the first transition, and dissociation of the dimer occurs during the second transition.

For EGST, the CSM signal shows a blue shift followed by a red shift as the dimeric intermediate is populated and then unfolds, and this effect becomes more pronounced at higher protein concentrations (Figure 6B). This suggests that one or more tryptophan residues are in a more hydrophobic environment in the intermediate than in the native state. Further, since the fluorescence intensity of the central plateau (Figure 6A) or turning point (Figure 6B) between the two transitions is affected by protein concentration, this suggests that the unfolding mechanism may involve at least two folding intermediates (one dimeric, one monomeric) with different spectral properties, the relative populations of which are shifted with protein concentration. Consistent with this, fitting of the data to a three-state model ($N_2 \leftrightarrow I_2 \leftrightarrow 2U$; see the Experimental section) gives different stability values at different protein concentrations (not shown), indicating that the three-state model ($N_2 \leftrightarrow I_2 \leftrightarrow 2U$) does not fully describe the unfolding mechanism and so the parameters obtained using this model will tend to underestimate the true stability of the protein [33]. However, any additional transitions are not sufficiently well resolved to allow fitting to a more complex model, and so the three-state model was used as the best approximation to describe the denaturation of EGST (see Table 2 and the Discussion below).

The equilibrium denaturation profile observed when using urea as a denaturant in place of GdmCl showed similar features (Figure 6C). This confirms that the observation of a complex equilibrium denaturation profile for EGST is not due to the effects of GdmCl as a salt.

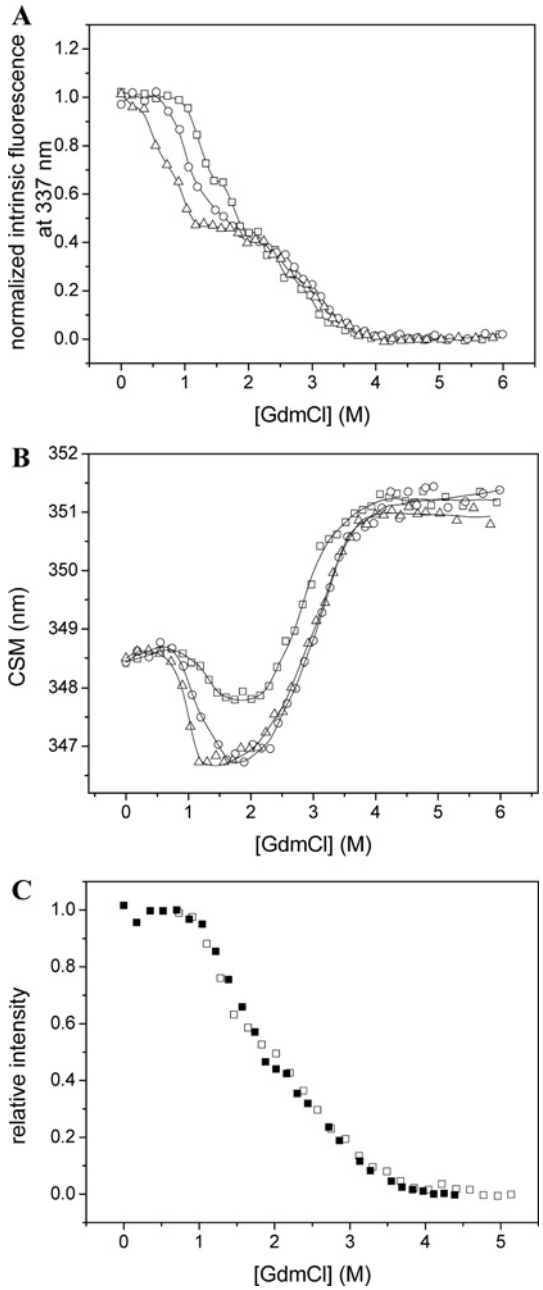

Figure 5 Comparison of GdmCl denaturation of EGST at different pH values

Unfolding (open symbols) and refolding (closed symbols) of 1 μM EGST was performed at pH 7.5 (□, ■), pH 8.0 (○) and pH 8.4 (△).The experimental conditions were as follows: Tris/HCl buffer, 50 mM; NaCl, 0.2 M; DTT, 1 mM; temperature, 25 °C. (**A**) Intrinsic fluorescence monitored at 337 nm after excitation at 280 nm. (**B**) The same data as in (**A**) represented as the CSM (see the Experimental section). (**C**) Comparison of unfolding and refolding of EGST using intrinsic fluorescence monitored at 337 nm after excitation at 280 nm at pH 7.5.

In order to investigate further the equilibrium unfolding mechanism, we used CD, enzymatic activity and binding of the hydrophobic dye ANS (which is often used to detect a population of partially folded intermediates [46]) as additional structural probes. As shown in Figure 7(A), when the unfolding transition was monitored using identical samples by fluorescence (at 337 nm, which monitors the global conformation of the protein) and CD (at 222 nm, which monitors helical secondary structure), the curves did not completely overlay within the second

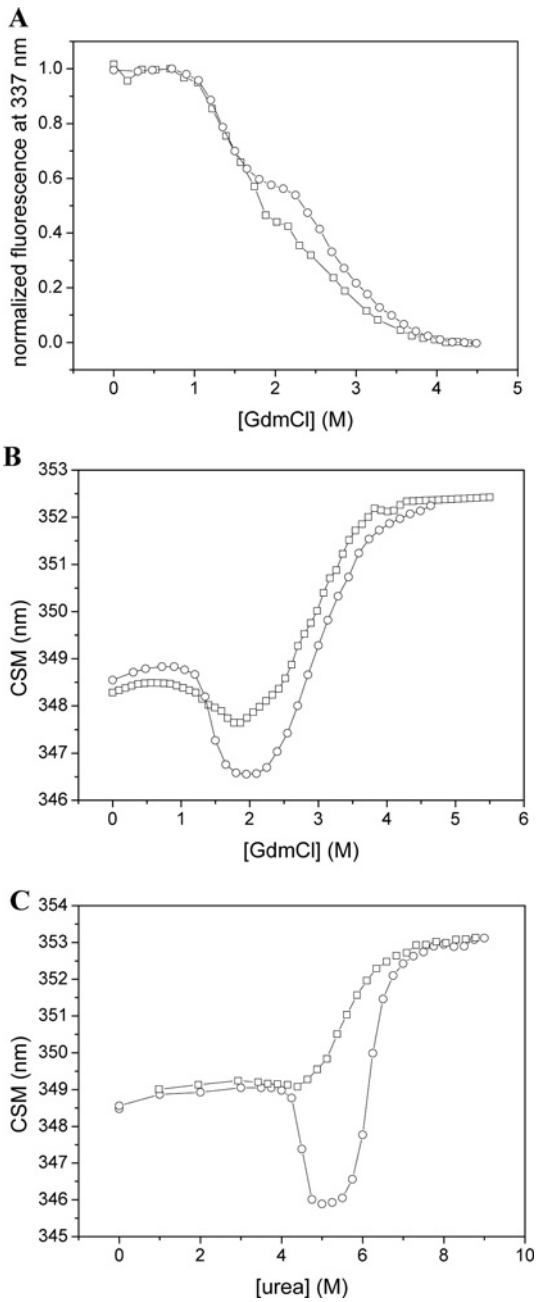

Figure 6 Effect of protein concentration on the EGST equilibrium denaturation profile in GdmCl and urea

The concentration of WT EGST was 1 μM (□) or 7 μM (○). The experimental conditions were as follows: temperature, 25 °C; pH, 7.5; buffer, 50 mM Tris/HCl; NaCl, 0.2 M; DTT, 1 mM. (**A**) Denaturation by GdmCl monitored by fluorescence at 337 nm or (**B**) fluorescence CSM; (**C**) denaturation by urea monitored by fluorescence CSM.

transition. Similarly, when urea was used as the denaturant, mismatch between the two curves was observed within the central plateau and second transition regions (Figure 7B). This is indicative of a population of an additional folding intermediate [43] and suggests that complete loss of tertiary structure precedes complete loss of secondary structure. When we examined changes in the ability to bind ANS during GdmCl denaturation (Figure 7C), a peak was observed which coincides with the first transition observed by CD (Figure 7A) or by fluorescence (Figures 7A and 7C), suggesting increased exposure of hydrophobic surface area in the dimeric intermediate. Loss of enzymatic activity preceded structural changes detected by other probes and fell steadily throughout the first transition (Figure 7C). This suggests that the partially folded intermediates of EGST are enzymatically inactive.

Comparison of structure and stability of WT and mutant EGST

The far-UV CD spectra of WT and mutant EGST are compared in Figure 8(A). The mutants C10A and H106A (continuous and broken curves in Figure 8A respectively), show a slight change in the far-UV CD spectrum in the region around 222 nm, indicating a slight change in α-helical content, whereas the more conservative mutations, C10S and H106F, are indistinguishable from the WT. The fluorescence CSM values for H106F are shifted to lower wavelength (Figure 8B), suggesting greater hydrophobic burial of one or more tryptophan residues in the folded structure of H106F compared with the WT.

The stability of the mutants was compared by GdmCl denaturation (Figure 8B). Compared with WT EGST, the mid-point of the first transition was shifted to slightly higher GdmCl concentration for C10A (and C10S) and to significantly lower GdmCl concentration for H106A (and H106F). In order to present the relative effects of these mutations in quantitative terms, we fitted the data to a three-state model and the results are shown in Table 2. The results suggest that mutation of Cys^{10} to alanine or serine stabilizes the protein. Whereas mutation of His^{106} to alanine (or phenylalanine) shifts the first transition to a lower GdmCl concentration, the change in overall stability of the protein is not significant and the H106F mutation seems in fact to stabilize the protein overall.

DISCUSSION

Structural analysis

EGST contains three tryptophan residues, namely Trp^{97}, Trp^{145} and Trp^{164} (Figure 2). Trp^{97} lies near the dimer interface. Trp^{145} is close to the surface of the protein, in the all-α-domain and near the linker between the two domains. Trp^{164} also lies within the all-α-domain, at the interface of the two domains, near the entrance to the catalytic cleft. The distribution of the tryptophan residues in the protein structure means that changes in intrinsic tryptophan fluorescence are expected to reflect the overall folding of the protein. The equivalent residues of Trp^{97} and Trp^{164} in PmGST (Figure 1) were investigated and Trp^{97} was found to make a greater contribution to intrinsic fluorescence than Trp^{164} [19].

Roles of Cys^{10} and His^{106} in catalysis

The present study demonstrates that residues Cys^{10} and His^{106} in EGST are directly involved in substrate binding and catalysis for the GST activity of EGST, consistent with the proximity of these resi-dues to the sulfonate group of the inhibitor glutathione sulfonate bound in the active site of EGST [22]. In the case of mutation of residue Cys^{10}, the K_m for GSH was observed to decrease (C10A > WT > C10S) as the polarity of the side chain increases (Ala < Cys < Ser), and the decrease in K_m was accompanied by an decrease in k_{cat} (Table 1). As the K_m roughly reflects the affinity of the substrate for the enzyme and k_{cat} represents the catalytic-centre activity ('turnover number'), the results suggest that the residue at position 10 is involved in binding of the substrate GSH, but that increased tightness of substrate binding may hamper product release and thus reduce the apparent activity of the enzyme. Given that activity is maintained (and in fact increased) in the C10A mutant, clearly a direct interaction between the Cys^{10} S^{γ} atom and the thiol group of GSH is not

Table 2 Thermodynamic parameters obtained from fitting of CSM using a three-state model

The conditions were as follows: temperature, 25 °C; buffer, 50 mM Tris/HCl, pH 7.5; NaCl, 0.2 M. Results are the mean ± S.E.M. for at least three independent measurements. The data were fitted to the model $N_2 \leftrightarrow I_2 \leftrightarrow 2U$ (see the text). $[GdmCl]_{1/2}$ is the midpoint and m is the slope of the transition. It should be noted that the parameters shown may underestimate the true stability of the EGST protein and its mutants owing to a population of further folding intermediates. However, as further transitions are insufficiently well resolved by any of the available structural probes, this three-state model offers the best approximation in the case of EGST. The '$_1$' and '$_2$' after the m, $[GdmCl]_{1/2}$ and ΔG values refer to the first and second transitions respectively. ΔG *is* the Gibbs free-energy change of transition.

EGST	m_1 (kJ · mol^{-1} · M^{-1})	m_2 (kJ · mol^{-1} · M^{-1})	$[GdmCl]_{1/2,1}$ (M)	$[GdmCl]_{1/2,2}$ (M)	ΔG_1 (kJ · mol^{-1})	ΔG_2 (kJ · mol^{-1})	ΔG_U (kJ · mol^{-1})
WT	10.9 ± 2.0	9.3 ± 1.7	1.4 ± 0.1	2.9 ± 0.1	15 ± 3	27 ± 5	42 ± 6
C10A	18.2 ± 0.4	12.8 ± 2.3	1.58 ± 0.06	2.90 ± 0.02	29 ± 2	37 ± 7	66 ± 7
C10S	19 ± 2	16 ± 1	1.52 ± 0.03	2.75 ± 0.03	29 ± 4	43 ± 3	73 ± 5
H106A	12.2 ± 5.2	11.8 ± 0.2	0.72 ± 0.03	3.06 ± 0.01	9 ± 4	36 ± 1	45 ± 4
H106F	16 ± 4	17 ± 1	0.4 ± 0.3	3.20 ± 0.04	7 ± 6	54 ± 3	61 ± 6

required for GST activity. Thus if Cys[10] plays a direct role in catalysis of GST activity, it is likely to be the amide N atom of residue Cys[10] that interacts with GSH. Interestingly, the activity towards CDNB of the human Omega-class enzyme GSTO1-1, which also has an active-site cysteine residue, is likewise increased by mutation to alanine [47].

The fact that the activity of H106F is lower than that of the WT, but higher than that of H106A, suggests that the aromatic ring is primarily responsible for the catalytic contribution of this residue, but that the charge and/or orientation of a histidine residue at position 106 provides an active site that is better optimized for activity.

None of the Cys[10] and His[106] mutations studied here fully abrogates the GST activity of EGST. This suggests that the overall fold and architecture of the protein, and the microenvironment of the catalytic cleft, allow for some plasticity in the choice of residue at this site. Further, as mutation of Cys[10] in particular can actually improve the catalytic activity of the enzyme, this suggests that the presence of a cysteine residue may contribute in ways other than providing optimal GST activity, as measured using the substrate CDNB.

In order to investigate further the role of residue Cys[10] in EGST, we tested for, and found, thiol:disulfide oxidoreductase activity for this enzyme that appeared to rely on the presence of Cys[10] (Figure 3). The closely related enzyme PmGST [7,17], as well as the Omega-class enzyme GSTO1-1 [13,47], both show thiol:disulfide oxidoreductase activity involving formation of a mixed disulfide with the active-site cysteine residue. Our tryptophan quenching data (Figure 4) show that Cys[10] of EGST can also form a mixed disulfide with its substrate GSH. Taken together, the sulfur atom of Cys[10] is essential for redox activity, but not for conjugating activity, consistent with the suggestion that the amide N atom of Cys[10] might play a role as a hydrogen-bond donor that stabilizes the negatively charged thiolate ion of GSH during the catalysis [22], whereas the redox activity involves formation of a mixed disulfide between the thiol sulfur atom of GSH and the S^{γ} atom of Cys[10].

Folding properties of EGST

Equilibrium unfolding experiments showed that the denaturation of EGST by chemical denaturants is a multi-step process. As shown in Figure 5(A), the stability of EGST decreases with increasing pH during the first transition. This may be due to increased electrostatic repulsion of charged residues as the pH is increased over this range. As the second transition shows no pH-dependence, this suggests that disruption of non-electrostatic interactions, for example dissociation of the dimer and/or disruption of the hydrophobic core, predominates at this stage. In fact, the structure of EGST (Protein Data Base entry 1a0f) indicates that the dimer interface has many electrostatic interactions. This is consistent with the observation that there are many bound water molecules near the subunit interface [22] and is similar to the case of GSTS1-1, a Sigma-class GST, where the interface of the two subunits of the dimer is relatively hydrophilic compared with mammalian GSTs [31]. This will tend to make the dissociation of the dimer pH-dependent. However, the observation of a blue shift in the CSM spectrum during the first transition, together with a peak in ANS binding (Figure 7C), suggests that significant structural rearrangement may take place during the course of denaturation. The result of a comparison of the different structural probes (Figures 6 and 7) indicates that EGST unfolds in a stepwise manner, involving population of at least two folding intermediates, one of which is dimeric. Taken together, the unfolding process can be described as follows:

$$N_2 \leftrightarrow (I_2 \leftrightarrow I) \leftrightarrow 2U$$

where I (a monomeric intermediate) and I_2 are in equilibrium and I_2 may have undergone significant rearrangement at the dimeric interface compared with the native dimeric state, N_2. The observation of a dimeric intermediate for EGST indicates that the protein derives a significant fraction of its overall stability from dimer formation.

This behaviour of EGST is very like that of yeast Ure2p, which also shows a complex denaturation profile with population of folding intermediates, including a dimeric intermediate that binds strongly to ANS [33]. However, despite the structural similarities between the proteins, their sequence identity is low and, unusually, Ure2p is predicted to use an asparagine residue (Asn[124]; located near the N-terminus of the globular GST-like domain of Ure2p) as the crucial catalytic residue [24]. Perhaps reflecting this lack of a consensus tyrosine, serine or cysteine residue in the active site, Ure2p shows GSH-dependent peroxidase activity [48], but shows no reactivity towards the standard GST substrate CDNB [49].

Contribution of Cys[10] and His[106] to the stability of EGST

Comparison of the equilibrium unfolding of mutant and WT EGST (Figure 8 and Table 2) indicates that mutation of Cys[10] to serine significantly stabilized the protein while causing little or no change to the WT structure. The less-conservative mutation C10A also significantly stabilized the protein, possibly accompanied by slight changes in local helical structure. On the other hand, His[106] does not contribute to the stability of the enzyme: mutation of the histidine to alanine had a negligible effect on stability, and replacement of histidine by phenylalanine actually stabilized the protein. H106A may cause slight changes in local helical

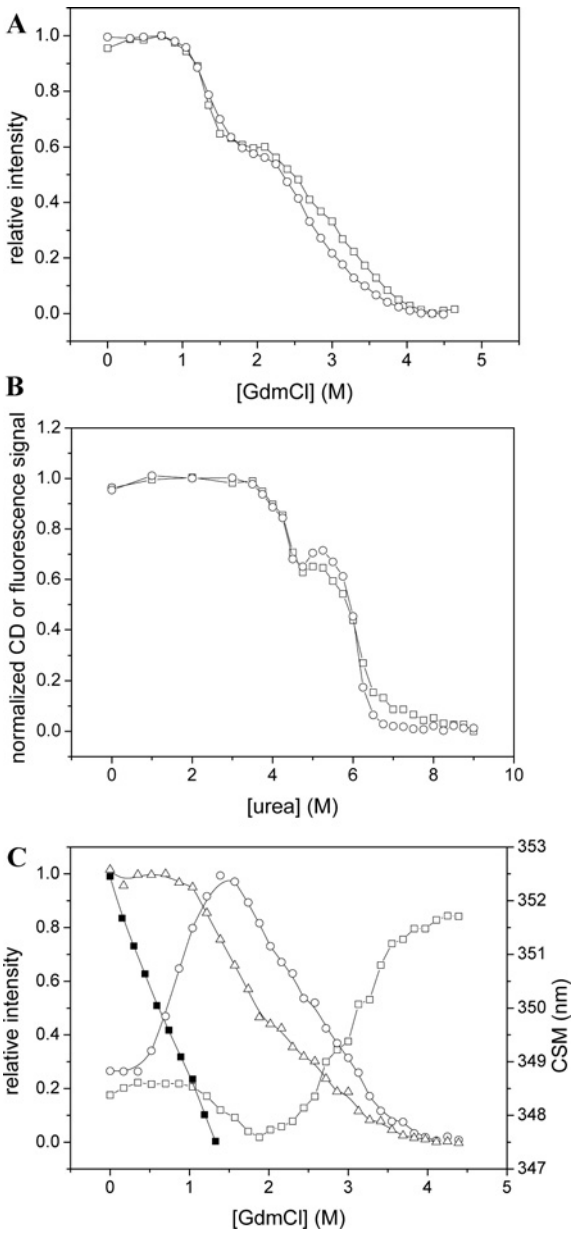

Figure 7 Comparison of different structural probes for the denaturation of WT EGST

The experimental conditions were as follows: temperature, 25 °C; pH, 7.5; buffer, 50 mM Tris/HCl; NaCl, 0.2 M; DTT, 1 mM. The Figure shows a comparison of EGST denaturation monitored by CD at 222 nm (□) and by intrinsic fluorescence at 337 nm (○) using GdmCl (**A**) or urea (**B**). The EGST concentration was 7 μM. (**C**) Comparison of GdmCl denaturation of EGST monitored by GST activity (■), ANS binding (○), intrinsic fluorescence at 337 nm (△) or fluorescence CSM (□). The EGST concentration was 1 μM. Activity measurements were performed as described in the Experimental section using GSH and CDNB concentrations of 1 mM.

structure, but without any significant change in overall protein conformation, and the mutation H106F may give rise to a change in the microenvironment of Trp^{164}, which is nearby in the folded structure.

Taken together with the results of the activity experiments, this indicates that the residue His^{106} plays a role in the GST activity of EGST, but is not important for protein stability. By contrast, the presence of a cysteine residue at position 10 is optimal for neither protein stability nor GST activity, suggesting that the presence

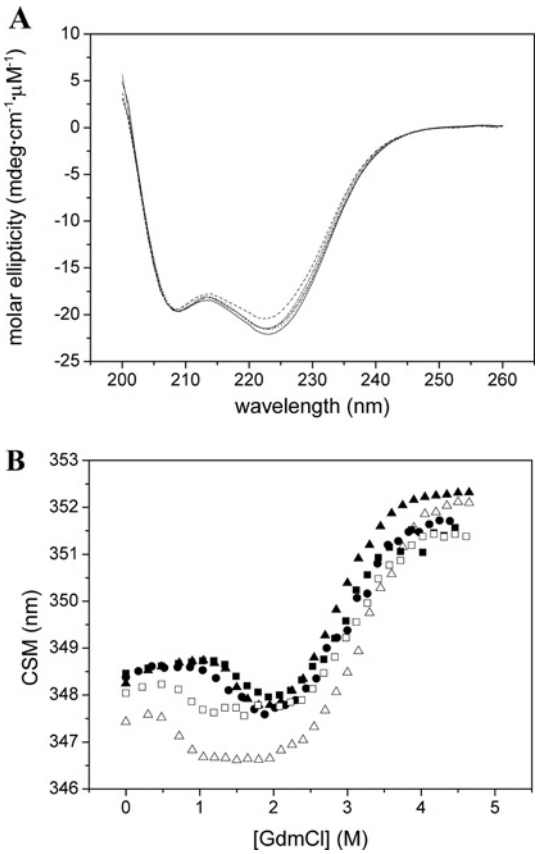

Figure 8 Comparison of structure and stability of WT EGST and its mutants

The experimental conditions were as follows: temperature, 25 °C; pH, 7.5; buffer, 50 mM Tris/HCl; NaCl, 0.2 M. (**A**) CD spectra of WT EGST (dotted line), C10A (——), H106A (– – – –), C10S (–·–·) and H106F (–··). The protein concentration was 30 μM. (**B**) GdmCl denaturation of WT EGST (●), C10A (■), C10S (▲), H106A (□) and H106F (△) monitored by fluorescence CSM. The protein concentration was 1 μM with 1 mM DTT. Abbreviation: mdeg, millidegree.

of a cysteine residue is related to its essential role in the redox activity of the enzyme.

Conclusions

The present study demonstrates the involvement of residues Cys^{10} and His^{106} in the catalytic activity of EGST and illustrates the flexibility of the GST scaffold and diversity of its active site, even among closely related organisms or protein structures. Mutation of the residue His^{106} caused a moderate decrease in activity, but a negligible effect on stability, a finding consistent with the similar importance of the equivalent residue His^{106} in the activity of the closely related PmGST [16]. The role of residue Cys^{10} is particularly interesting. The equivalent residue, Cys^{10}, is observed to be covalently linked to a GSH molecule in PmGST [7], which is ascribed to a redox role for the enzyme [17], whereas no indication had yet been found for such a role for this residue in EGST [22,23]. The present study demonstrates that Cys^{10} in EGST is also involved in a redox role and, similarly, we find evidence for formation of a mixed disulphide with GSH, suggesting this may represent an intermediate in the reaction cycle. This in turn accounts for our finding that, in terms of the GST activity of EGST, the presence of a cysteine residue at position 10 is neither optimized for catalysis nor for protein stability.

ACKNOWLEDGMENTS

We thank Professor Jun-Mei Zhou (National Laboratory of Biomacromolecules, Institute of Biophysics, Chinese Academy of Sciences, Beijing, China) for much help, advice and encouragement.

FUNDING

This work was supported by the Natural Science Foundation of China [grant nos. 30470363, 30620130109, 30670428 and 30870482]; the Chinese Ministry of Science and Technology [grant nos. 2006CB500703, 2006CB910903]; and the Chinese Academy of Sciences Knowledge Innovation Project [grant no. KSCX2-YW-R-119]. X.-Y.W. was supported by a post-doctoral award from the Wang Kuancheng Foundation.

REFERENCES

1 Armstrong, R. N. (1997) Structure, catalytic mechanism and evolution of the glutathione transferases. Chem. Res. Toxicol. **10**, 2–18
2 Sheehan, D., Meade, G., Foley, V. M. and Dowd, C. A. (2001) Structure, function and evolution of glutathione transferases: implications for classification of non-mammalian members of an ancient enzyme superfamily. Biochem. J. **360**, 1–16
3 Mannervik, B., Board, P. G., Hayes, J. D., Listowsky, I. and Pearson, W. R. (2005) Nomenclature for mammalian soluble glutathione transferases. Methods Enzymol. **401**, 1–8
4 Hayes, J. D., Flanagan, J. U. and Jowsey, I. R. (2005) Glutathione transferases. Annu. Rev. Pharmacol. Toxicol. **45**, 51–88
5 Frova, C. (2006) Glutathione transferases in the genomics era: new insights and perspectives. Biomol. Eng. **23**, 149–169
6 Mannervik, B., Alin, P., Guthenberg, C., Jensson, H., Tahir, M. K., Warholm, M. and Jornvall, H. (1985) Identification of three classes of cytosolic glutathione transferase common to several mammalian species: correlation between structural data and enzymatic properties. Proc. Natl. Acad. Sci. U.S.A. **82**, 7202–7206
7 Rossjohn, J., Polekhina, G., Feil, S. C., Allocati, N., Masulli, M., De, I. C. and Parker, M. W. (1998) A mixed disulfide bond in bacterial glutathione transferase: functional and evolutionary implications. Structure **6**, 721–734
8 Enayati, A. A., Ranson, H. and Hemingway, J. (2005) Insect glutathione transferases and insecticide resistance. Insect Mol. Biol. **14**, 3–8
9 Ranson, H., Rossiter, L., Ortelli, F., Jensen, B., Wang, X., Roth, C. W., Collins, F. H. and Hemingway, J. (2001) Identification of a novel class of insect glutathione S-transferases involved in resistance to DDT in the malaria vector *Anopheles gambiae*. Biochem. J. **359**, 295–304
10 Board, P. G., Baker, R. T., Chelvanayagam, G. and Jermiin, L. S. (1997) Zeta, a novel class of glutathione transferases in a range of species from plants to humans. Biochem. J. **328**, 929–935
11 Meyer, D. J., Coles, B., Pemble, S. E., Gilmore, K. S., Fraser, G. M. and Ketterer, B. (1991) Theta, a new class of glutathione transferases purified from rat and man. Biochem. J. **274**, 409–414
12 Ji, X., von Rosenvinge, E. C., Johnson, W. W., Tomarev, S. I., Piatigorsky, J., Armstrong, R. N. and Gilliland, G. L. (1995) Three-dimensional structure, catalytic properties and evolution of a Sigma class glutathione transferase from squid, a progenitor of the lens S-crystallins of cephalopods. Biochemistry **34**, 5317–5328
13 Board, P. G., Coggan, M., Chelvanayagam, G., Easteal, S., Jermiin, L. S., Schulte, G. K., Danley, D. E., Hoth, L. R., Griffor, M. C., Kamath, A. V. et al. (2000) Identification, characterization and crystal structure of the Omega class glutathione transferases. J. Biol. Chem. **275**, 24798–24806
14 Mignogna, G., Allocati, N., Aceto, A., Piccolomini, R., Di, I. C., Barra, D. and Martini, F. (1993) The amino acid sequence of glutathione transferase from *Proteus mirabilis*, a prototype of a new class of enzymes. Eur. J. Biochem. **211**, 421–425
15 Casalone, E., Allocati, N., Ceccarelli, I., Masulli, M., Rossjohn, J., Parker, M. W. and Di, I. C. (1998) Site-directed mutagenesis of the *Proteus mirabilis* glutathione transferase B1-1 G-site. FEBS Lett. **423**, 122–124
16 Allocati, N., Casalone, E., Masulli, M., Polekhina, G., Rossjohn, J., Parker, M. W. and Di, I. C. (2000) Evaluation of the role of two conserved active-site residues in Beta class glutathione S-transferases. Biochem. J. **351**, 341–346
17 Caccuri, A. M., Antonini, G., Allocati, N., Di, I. C., De, M. F., Innocenti, F., Parker, M. W., Masulli, M., Lo, B. M., Turella, P., Federici, G. and Ricci, G. (2002) GSTB1-1 from *Proteus mirabilis*: a snapshot of an enzyme in the evolutionary pathway from a redox enzyme to a conjugating enzyme. J Biol. Chem. **277**, 18777–18784
18 Allocati, N., Favaloro, B., Masulli, M., Alexeyev, M. F. and Di, I. C. (2003) *Proteus mirabilis* glutathione S-transferase B1-1 is involved in protective mechanisms against oxidative and chemical stresses. Biochem. J. **373**, 305–311
19 Allocati, N., Masulli, M., Pietracupa, M., Favaloro, B., Federici, L. and Di, I. C. (2005) Contribution of the two conserved tryptophan residues to the catalytic and structural properties of *Proteus mirabilis* glutathione S-transferase B1-1. Biochem. J. **385**, 37–43
20 Allocati, N., Masulli, M., Pietracupa, M., Federici, L. and Di, I. C. (2006) Evolutionarily conserved structural motifs in bacterial GST (glutathione S-transferase) are involved in protein folding and stability. Biochem. J. **394**, 11–17
21 Nishida, M., Kong, K. H., Inoue, H. and Takahashi, K. (1994) Molecular cloning and site-directed mutagenesis of glutathione S-transferase from *Escherichia coli*. The conserved tyrosyl residue near the N terminus is not essential for catalysis. J. Biol. Chem. **269**, 32536–32541
22 Nishida, M., Harada, S., Noguchi, S., Satow, Y., Inoue, H. and Takahashi, K. (1998) Three-dimensional structure of *Escherichia coli* glutathione S-transferase complexed with glutathione sulfonate: catalytic roles of Cys^{10} and His^{106}. J. Mol. Biol. **281**, 135–147
23 Rife, C. L., Parsons, J. F., Xiao, G., Gilliland, G. L. and Armstrong, R. N. (2003) Conserved structural elements in glutathione transferase homologues encoded in the genome of *Escherichia coli*. Proteins **53**, 777–782
24 Bousset, L., Belrhali, H., Janin, J., Melki, R. and Morera, S. (2001) Structure of the globular region of the prion protein Ure2 from the yeast *Saccharomyces cerevisiae*. Structure. **9**, 39–46
25 Lian, H. Y., Jiang, Y., Zhang, H., Jones, G. W. and Perrett, S. (2006) The yeast prion protein Ure2: structure, function and folding. Biochim. Biophys. Acta **1764**, 535–545
26 Dirr, H. W. and Reinemer, P. (1991) Equilibrium unfolding of class Pi glutathione S-transferase. Biochem. Biophys. Res. Commun. **180**, 294–300
27 Alves, C. S., Kuhnert, D. C., Sayed, Y. and Dirr, H. W. (2006) The intersubunit lock-and-key motif in human glutathione transferase A1-1: role of the key residues Met^{51} and Phe^{52} in function and dimer stability. Biochem. J. **393**, 523–528
28 Aceto, A., Caccuri, A. M., Sacchetta, P., Bucciarelli, T., Dragani, B., Rosato, N., Federici, G. and Di, I. C. (1992) Dissociation and unfolding of Pi-class glutathione transferase. Evidence for a monomeric inactive intermediate. Biochem. J. **285**, 241–245
29 Sacchetta, P., Pennelli, A., Bucciarelli, T., Cornelio, L., Amicarelli, F., Miranda, M. and Di, I. C. (1999) Multiple unfolded states of glutathione transferase bbGSTP1-1 by guanidinium chloride. Arch. Biochem. Biophys. **369**, 100–106
30 Hornby, J. A., Luo, J. K., Stevens, J. M., Wallace, L. A., Kaplan, W., Armstrong, R. N. and Dirr, H. W. (2000) Equilibrium folding of dimeric class mu glutathione transferases involves a stable monomeric intermediate. Biochemistry **39**, 12336–12344
31 Stevens, J. M., Hornby, J. A., Armstrong, R. N. and Dirr, H. W. (1998) Class sigma glutathione transferase unfolds via a dimeric and a monomeric intermediate: impact of subunit interface on conformational stability in the superfamily. Biochemistry **37**, 15534–15541
32 Galani, D., Fersht, A. R. and Perrett, S. (2002) Folding of the yeast prion protein Ure2: kinetic evidence for folding and unfolding intermediates. J. Mol. Biol. **315**, 213–227
33 Zhu, L., Zhang, X. J., Wang, L. Y., Zhou, J. M. and Perrett, S. (2003) Relationship between stability of folding intermediates and amyloid formation for the yeast prion Ure2p: a quantitative analysis of the effects of pH and buffer system. J. Mol. Biol. **328**, 235–254
34 Abdalla, A. M. and Hamed, R. R. (2006) Multiple unfolding states of glutathione transferase from *Physa acuta* (Gastropoda: Physidae). Biochem. Biophys. Res. Commun. **340**, 625–632
35 Wallace, L. A., Burke, J. and Dirr, H. W. (2000) Domain-domain interface packing at conserved Trp-20 in class Alpha glutathione transferase impacts on protein stability. Biochim. Biophys. Acta **1478**, 325–332
36 Hornby, J. A., Codreanu, S. G., Armstrong, R. N. and Dirr, H. W. (2002) Molecular recognition at the dimer interface of a class mu glutathione transferase: role of a hydrophobic interaction motif in dimer stability and protein function. Biochemistry **41**, 14238–14247
37 Hegazy, U. M., Mannervik, B. and Stenberg, G. (2004) Functional role of the lock and key motif at the subunit interface of glutathione transferase p1-1. J. Biol. Chem. **279**, 9586–9596
38 Wongsantichon, J. and Ketterman, A. J. (2006) An intersubunit lock-and-key 'clasp' motif in the dimer interface of Delta class glutathione transferase. Biochem. J. **394**, 135–144
39 Miroux, B. and Walker, J. E. (1996) Over-production of proteins in *Escherichia coli*: mutant hosts that allow synthesis of some membrane proteins and globular proteins at high levels. J. Mol. Biol. **260**, 289–298
40 Gill, S. C. and von Hippel, P. H. (1989) Calculation of protein extinction coefficients from amino acid sequence data. Anal. Biochem. **182**, 319–326
41 Habig, W. H. and Jakoby, W. B. (1981) Assays for differentiation of glutathione S-transferases. Methods Enzymol. **77**, 398–405

42 Axelsson, K., Eriksson, S. and Mannervik, B. (1978) Purification and characterization of cytoplasmic thioltransferase (glutathione:disulfide oxidoreductase) from rat liver. Biochemistry **17**, 2978–2984
43 Pace, C. N. and Scholtz, J. M. (1997) Measuring the conformational stability of a protein. In Protein Structure: A Practical Approach, 2nd edn (T. E. Creighton, ed.), p. 309, IRL Press/Oxford University Press, Oxford
44 Silva, J. L., Miles, E. W. and Weber, G. (1986) Pressure dissociation and conformational drift of the β dimer of tryptophan synthase. Biochemistry **25**, 5780–5786
45 Ruddock, L. W., Hirst, T. R. and Freedman, R. B. (1996) pH-dependence of the dithiol-oxidizing activity of DsbA (a periplasmic protein thiol:disulphide oxidoreductase) and protein disulphide-isomerase: studies with a novel simple peptide substrate. Biochem. J. **315**, 1001–1005
46 Fink, A. L. (1995) Compact intermediate states in protein folding. Annu. Rev. Biophys. Biomol. Struct. **24**, 495–522
47 Whitbread, A. K., Masoumi, A., Tetlow, N., Schmuck, E., Coggan, M. and Board, P. G. (2005) Characterization of the Omega class of glutathione transferases. Methods Enzymol. **401**, 78–99
48 Bai, M., Zhou, J. M. and Perrett, S. (2004) The yeast prion protein Ure2 shows glutathione peroxidase activity in both native and fibrillar forms. J. Biol. Chem. **279**, 50025–50030
49 Coschigano, P. W. and Magasanik, B. (1991) The URE2 gene product of *Saccharomyces cerevisiae* plays an important role in the cellular response to the nitrogen source and has homology to glutathione S-transferases. Mol. Cell Biol. **11**, 822–832
50 Delano, W. L. (2002) The PyMOL User's Manual, DeLano Scientific, Palo Alto

Received 19 December 2007/19 August 2008; accepted 9 September 2008
Published as BJ Immediate Publication 9 September 2008, doi:10.1042/BJ20071702